Development of a measurement system for noise and vibration of combine harvester

Deniz Yılmaz*, Mehmet Emin Gökduman

(*Department of Agricultural Machinery & Technology Engineering, Faculty of Agriculture ,
Isparta University of Applied Sciences, Isparta, Turkey*)

Abstract: Combine harvesters are important in that grain and legumes directly affect the production economy. On the other hand, it forms an important branch of the agricultural machinery sector. There are many unknown constraints on machines when harvesting with a combine harvester, including the noise and vibration that occur in the combine harvester thresher. This study aims to analyze noise and vibration in conventional combine harvesters using sensors. Two accelerometers were installed on each side of the concave and two microphones were used to register the noise of the threshing process. The result showed that effects of machine speeds (3.5 km/h, 4.5 km/h and 5.5 km/h) and rotor speeds (950 r/min, 850 r/min and 950 r/min) were significantly important for the mean range values of the left and right accelerometer in the *X*, *Y* and *Z* direction. The machine's speed and rotor speed were not significantly important for the mean range values of the left and right microphones.

Keywords: measurement, combine harvester, sensors, noise, vibration
DOI: 10.25165/j.ijabe.20201306.5554

Citation: Yılmaz D, Gökduman M E. Development of a measurement system for noise and vibration of combine harvester. Int J Agric & Biol Eng, 2020; 13(6): 104–108.

1 Introduction

Harvesting is the process of collecting crops from the field and separating the grain from the crop. Many machine types are used in harvesting because of the large difference in the crop types for which they are used. Combine harvesters are large, complex machines sent to all corners of the world to harvest many different crops under all possible environmental conditions. Wide varieties of measures have been used to assess combine harvester performance[1-3]. Combine harvesting is a highly uncertain process that requires sensors that can extract on-the-go information throughout the process[4]. During harvesting, excessive vibrations on the combine cutting platform can increase grain loss, reduce the combine's lifetime, and affect both working precision and driver comfort[5,6].

The important issues for tractor drivers who operate harvesters particularly for farm and industrial machinery designers are: noise, humidity, temperature, air cleanliness, and vibration levels. Inadequate design objectives in any of these factors can create serious problems in the operator's ability to perform efficiently[6].

A common design objective among engineers (and a common research objective for scientists) is to identify the sources and volumes of noises and determine their impact on system performance[7].

However, the positions and quality of available measurement devices are limited by practical restrictions, economic concerns, and harsh environments, rendering combine process improvements such as grain loss control, engine load control, and threshing controllers a challenge in the design of combine automation systems[8].

Examining the effects of vibrations and noise requires that the working conditions of combine harvesters (as machine and rotor speeds) be monitored by sensors. Effectively studying the effects of vibrations and noise requires examining combine harvesters with sensors that monitor the operational working conditions.

The objective of this study is to investigate noise and vibration in conventional combine harvesters using sensors.

2 Materials and methods

2.1 Materials

A Laverda 225 Rev conventional combine harvester was used in this study. This machine is used to harvest wheat, barley, and corn in the Sandıkli region of Turkey. Figure 1 presents the main separation elements in a conventional Laverda 225 Rev combine harvester.

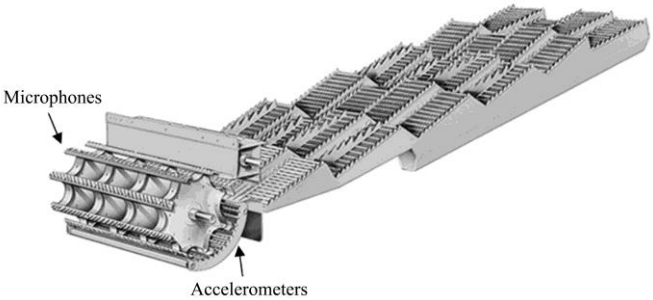

Figure 1 Overview of the main separation elements in a conventional combine harvester

Hardware and software are used to determine sensor values in conventional combine harvesters. The hardware used in this measurement setup (as shown in Figure 2) consists of, two accelerometers, two microphones, one signal-collection box, one

Received date: 2019-11-28 **Accepted date:** 2020-09-20

Biographies: Mehmet Emin Gökduman, PhD candidate, Research Assistant, research interests: combine harvester, agriculture machinery, harvesting technology, Email: mehmetgokduman@isparta.edu.tr .

***Corresponding author: Deniz Yilmaz,** PhD, Professor, research interests: combine harvester, harvesting technology, agriculture machinery. Department of Agricultural Machinery & Technology Engineering, Isparta University of Applied Sciences, Isparta, Turkey. Tel: +90-532-5683778, Email: denizyilmaz@isparta.edu.tr.

card, and one laptop.

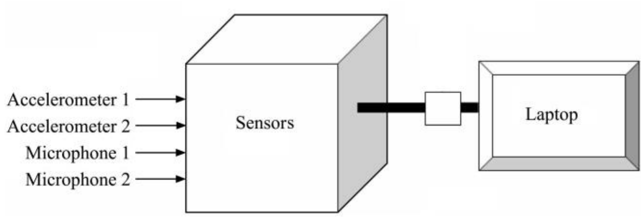

Figure 2 Hardware of sensor system

Many methods have been proposed to excite the vibrations of structural elements and thus evaluate the sensor measurement performance[9]. Most sensors, such as accelerometers, depend on receiving mechanical wave propagations either on or inside the structure[9,10]. In this study, accelerometers measured the dynamic impact of the machine feeding on the concave. This study used accelerometers that measure vibrations in the *X*, *Y*, and *Z* directions for actual force evaluation[11-13] on the concave. They were attached to the concave on either side of combine harvester as presented in Figure 3. Figure 4 shows the *X*, *Y* and *Z* directions for each accelerometer installed on the concave. Table 1 summarizes the features of the used accelerometers.

Figure 3 Placement of the accelerometers on both sides of the combine harvester

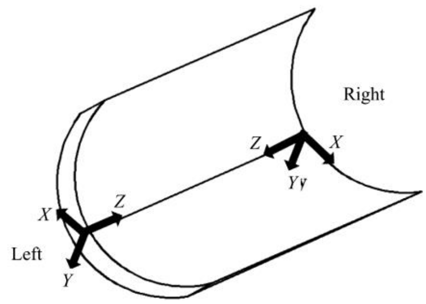

Figure 4 *X*, *Y*, *Z* direction of accelerometer in both sides of combine harvester

Table 1 Features of the accelerometer used

Features	Values
Parameters	Tri-Axial
Span/g	4±5%
Sensitivity/mV g^{-1}	400±5%
Bandwidth/Hz	DC–100±5%
Noise density/rms*	3
Orientation	Tri-Axial
Span output/V	±2.0±0.1 (+25℃),
Alignment/(°)	±2
Transverse sensitivity**	±3.5
Temperature range/℃	0 to +70
Shock/g	500 Powered, 2000 Unpowered
Supply voltage/V	+5±0.25
Functional range/V	+5±1
Supply Current/mA	10

Note: * rms = root mean square; ** Transverse Sensitivity is error measured in the primary axis output created by forces induced in the orthogonal axis.

As shown in Figure 5, two microphones were placed on either side of the combine under the cab and near the threshing drum to measure the noise and sound of the threshing process under different machine settings. Table 2 summarizes the features of the used microphones.

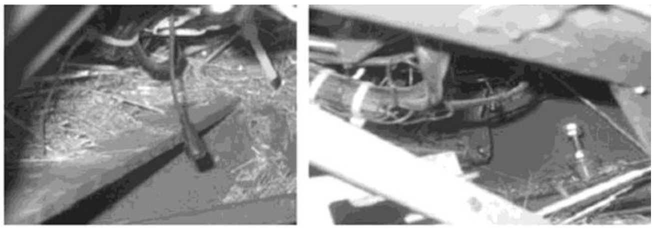

Figure 5 Microphones on both sides of the combine harvester

Table 2 Features of the used microphones

Features	Values
Frequency/Hz	50-17000
Amplifier/mV·Pa^{-1}·kHz^{-1}	5/1
Impedance/Ω	500
Maximum decibels/Db	130
Signal/dB	>40
Dimension/mm	ø12.2×4.6

A sensors box was constructed to collect the measured signals of the two accelerometers and two microphones. These four inputs were gathered on the green card. From that card, the signals were transferred to the Card in the measurement computer. The signal-collecting box was connected to every necessary input and the Card took the output to the measurement computer. The Matlab® software program was used to process the data afterward. The sensor signals were measured at a 5 Hz sample rate.

2.2 Methods

Before going into the field, resonance measurements were done on the concave. According to the results of the measurements the values were in the range of 20-100 kHz. The wheat experiments were done in June 2016. The field had no slope variations, so only one-way measurements were taken. The three machine speeds were 3.5, 4.5, and 5.5 km/h, used in several combinations with the three rotor speeds (750 r/min, 850 r/min, and 950 r/min) (Table 3). All experiments were done with three repetitions (*a*, *b*, *c*). The concave clearance was 11 mm. Each experiment took between 80 s and 120 s. A box was installed under the harvesting combine that could be dropped by pushing a button in the cab. The material that is thrown out at the back of the machine was collected in the dropped box.

Table 3 Explanation of the symbols

Symbol	Explanation
*Z*1	Machine speed: 3.5 km·h^{-1}
*Z*2	Machine speed: 4.5 km·h^{-1}
*Z*3	Machine speed: 5.5 km·h^{-1}
*Y*1	Rotor speed: 750 r·min^{-1}
*Y*2	Rotor speed: 850 r·min^{-1}
*Y*3	Rotor speed: 950 r·min^{-1}
a, *b*, *c*	Repetitions of the experiment

3 Results and discussion

The signals were measured while the machine was harvesting. Figure 6 consists of three plots of the signals. The *X*-direction is time in seconds, and *Y*-direction is the voltage value of the signal. The first two plots show the vibration signals of the accelerometers attached to both sides of the concave. The mean value is already subtracted from the signals. The sound in the neighborhood of the threshing drum on the left and right sides of the machine is shown in the third plot in Figure 6.

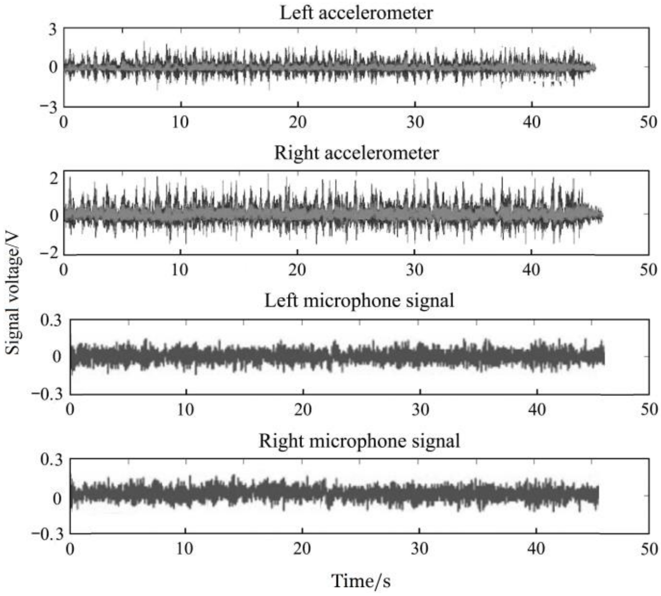

Figure 6 Plot of the signals measured while the machine is harvesting

In Figure 7, a screenshot of the spectral analysis done on the resampled accelerometer signals is shown. In the first, the resampled signal is shown, from which the mean value is subtracted. Plot No. 2 is the result of the spectral analysis done on No. 1. For each moment, the amplitude of all the frequencies was calculated and plotted in a three-dimensional graph. The *X*-direction is time, *Y*-direction presents all the frequencies, and *Z*-direction (height above the plain) illustrates how much of each frequency is present in the signal. This height is shown in a color code that is explained in No. 3. Screens 4 and 5 are further visualizations of the spectral analysis. In No. 2, a horizontal and a vertical line are shown. The amplitude of each frequency present in the signal at a sudden time, selected by the vertical line, is plotted in screen 4. Screen 5 is the amplitude of a certain frequency, selected by the horizontal line, and it is present in the signal as a function of the time. Finally, in No. 6, the selected time and frequency are shown, together with the amplitude of that frequency.

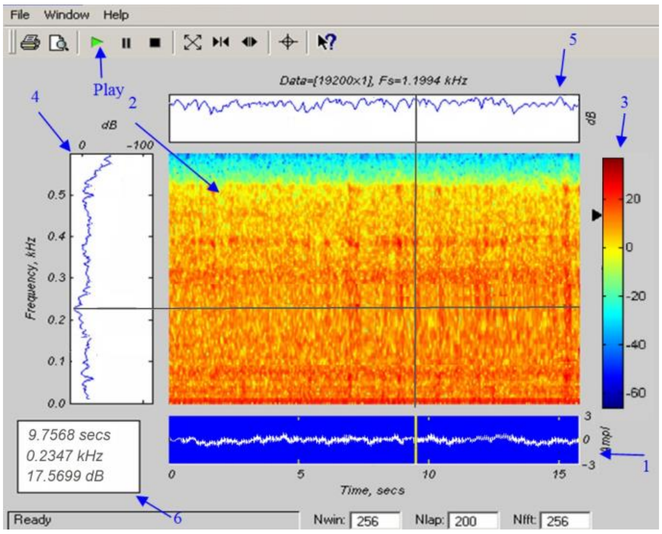

Figure 7 An example of spectral analysis of accelerometer signals

Data were analyzed using the Statistical Analysis System, Factorial General Linear Model (GLM) procedure (SAS 1995), and Duncan's multiple-range tests were used to identify significantly different means within dependent variables. In all the experiments, when the machine speed was set to *Z*1, *Z*2 and *Z*3, the rotor speed was set to 850 r/min. When the rotor speed is set to *Y*1, *Y*2 and *Y*3, the machine speed was set to 4.5 km/h. The results of the mean range values of the left accelerometer in the *X* direction are given in Table 4.

Table 4 Mean range values of the left accelerometer in the *X* direction (dB)

Machine speed**/km h^{-1}			Rotor speed**/r min^{-1}		
*Z*1 (3.5)	*Z*2 (4.5)	*Z*3 (5.5)	*Y*1 (750)	*Y*2 (850)	*Y*3 (950)
0.9837c ± 0.115	1.3295b ± 0.125	1.6558a ± 0.114	1.1188b ± 0.132	1.1258b ± 0.112	1.4488a ± 0.170

Note: Means within a group followed by same letter are not significantly different: $p = 0.01$ by Duncan's multiple range tests. **$p < 0.01$.

As can be seen in Table 4, the effects of the machine speed and rotor speed were significantly important on the mean range values of the left accelerometer in the *X* direction ($p<0.01$). The mean range value of the left accelerometer in the *X* direction on Z3 machine speed (1.6558 dB) was significantly higher than those of *Z*1 and *Z*2. In *Y*3 rotor speed, the mean range value of the left accelerometer in the *X* direction was significantly higher than those in *Y*1 and *Y*2 rotor speeds.

The results of the mean range values of the left accelerometer in *Y* direction are given in Table 5. The effects of machine speed and rotor speed were significantly important for the mean range values of the left accelerometer in *Y* direction ($p<0.01$). The mean range value of the left accelerometer in *Y* direction on *Z*1 machine speed (1.3594 dB) was significantly lower than that of *Z*2 and *Z*3 machine speeds. In *Y*1 rotor speed, the mean range value of the left accelerometer in *Y* direction (1.9010 dB) was significantly higher as compared with those of *Y*2 and *Y*3 rotor speeds.

Table 5 Mean range values of the left accelerometer in *Y* direction (dB)

Machine speed**/km h^{-1}			Rotor speed**/r min^{-1}		
*Z*1 (3.5)	*Z*2 (4.5)	*Z*3 (5.5)	*Y*1 (750)	*Y*2 (850)	*Y*3 (950)
1.3594b ± 0.112	1.9059a ± 0.136	1.8854a ± 0.154	1.9010a ± 0.123	1.5643b ± 0.128	1.5764b ± 0.142

Note: Means within a group followed by same letter are not significantly different: $p = 0.01$ by Duncan's multiple range tests. **$p < 0.01$, *$p < 0.05$.

The results of the mean range values of the left accelerometer in *Z* direction are given in Table 6. As seen in Table 6, the effects of machine speed and rotor speed were significantly important for the mean range values of the left accelerometer in *Z* direction ($p<0.05$). The mean range value of the left accelerometer in *Z* direction on *Z3* machine speed (0.9634 dB) was significantly higher than those of *Z*1 and *Z*2 machine speeds. The mean range value of the left accelerometer in *Z* direction for *Y*1 rotor speed (0.9236 dB) was significantly higher than those of *Y*2 and *Y*3 rotor speeds.

The results of the right accelerometer's mean range values in the *X* direction are given in Table 7. The effect of machine speed was significantly important for the mean range values of the right accelerometer in the *X* direction ($p<0.01$). The mean range value of the right accelerometer in the *X* direction on *Z*1 machine speed

(3.2654 dB) was significantly higher than those of *Z*2 and *Z*3 machine speeds.

Table 6 Mean range values of the left accelerometer in *Z* direction (dB)

Machine speed**/km h^{-1}			Rotor speed**/r min^{-1}		
*Z*1 (3.5)	*Z*2 (4.5)	*Z*3 (5.5)	*Y*1 (750)	*Y*2 (850)	*Y*3 (950)
0.8602b ± 0.042	0.9279ab ± 0.038	0.9634a ± 0.063	0.9236a ± 0.087	0.7245b ± 0.032	0.8625ab ± 0.042

Note: Means within a group followed by same letter are not significantly different: $p = 0.01$ and $p = 0.05$ by Duncan's multiple range tests. $^{**}p < 0.01$, $^{*}p < 0.05$.

Table 7 Mean range values of the right accelerometer in the *X* direction (dB)

Machine speed**/km h^{-1}			Rotor speed**/r min^{-1}		
*Z*1 (3.5)	*Z*2 (4.5)	*Z*3 (5.5)	*Y*1 (750)	*Y*2 (850)	*Y*3 (950)
3.2654^a ± 0.153	2.5326^b ± 0.123	2.4650^b ± 0.155	1.8452^a ± 0.123	1.8560^a ± 0.210	1.9638^a ± 0.223

Note: Means within a group followed by same letter are not significantly different: $p = 0.01$ by Duncan's multiple range tests. $^{**}p < 0.01$, $^{*}p < 0.05$.

The results of the mean range values of the right accelerometer in *Y* direction are given in Table 8. As seen in Table 8, the effects of machine and rotor speeds were significantly important for the mean range values of the right accelerometer in *Y* direction (p<0.01). The mean range value of the right accelerometer in Y direction for *Z*1 machine speed (3.0256 dB) was significantly higher as compared to that of *Z*2 and *Z*3 machine speeds. The mean range value of the right accelerometer in *Y* direction at *Y*3 rotor speed (3.5250 dB) was significantly higher than those of *Y*1 and *Y*2 rotor speeds.

Table 8 Mean range values of the right accelerometer in *Y* direction (dB)

Machine speed**/km h^{-1}			Rotor speed**/r min^{-1}		
*Z*1 (3.5)	*Z*2 (4.5)	*Z*3 (5.5)	*Y*1 (750)	*Y*2 (850)	*Y*3 (950)
3.0256^a ± 0.122	2.6523^b ± 0.196	2.6973^b ± 0.241	2.8911^{ab} ± 0.366	1.9747^b ± 0.356	3.5250^a ± 0.311

Note: Means within a group followed by same letter are not significantly different: $p = 0.01$ and $p = 0.05$ by Duncan's multiple range tests. $^{**}p < 0.01$, $^{*}p < 0.05$.

The results of the mean range values of the right accelerometer in *Z* direction are given in Table 9. The effects of machine speed and rotor speed were significantly important for the mean range values of the right accelerometer in *Z* direction (p<0.05). The mean range value of the right accelerometer in *Z* direction on *Z*3 machine speed (0.8941 dB) was significantly higher than those of *Z*1 and *Z*2 machine speeds. The mean range value of the right accelerometer in Z direction at *Y*2 rotor speed (0.6947 dB) was significantly lower as compared with those of *Y*1 and *Y*3 rotor speeds.

Table 9 Mean range values of the right accelerometer in *Z* direction (dB)

Machine speed**/km h^{-1}			Rotor speed**/r min^{-1}		
*Z*1 (3.5)	*Z*2 (4.5)	*Z*3 (5.5)	*Y*1 (750)	*Y*2 (850)	*Y*3 (950)
0.6277^b ± 0.021	0.7874^{ab} ± 0.033	0.8941^a ± 0.056	0.8267^a ± 0.032	0.6947^b ± 0.041	0.7822^a ± 0.049

Note: Means within a group followed by same letter are not significantly different: $p = 0.01$ and $p = 0.05$ by Duncan's multiple range tests. $^{**}p < 0.01$, $^{*}p < 0.05$.

The results of the mean range values of the left microphone are given in Table 10. Table 10 shows that the effects of machine speed and rotor speed were not significantly important for the mean range values of the left microphone.

Table 10 Mean range values of left microphone

Machine speed**/km h^{-1}			Rotor speed**/r min^{-1}		
*Z*1 (3.5)	*Z*2 (4.5)	*Z*3 (5.5)	*Y*1 (750)	*Y*2 (850)	*Y*3 (950)
0.3107^a ± 0.011	0.3054^a ± 0.008	0.3078^a ± 0.006	0.3079^a ± 0.018	0.3069^a ± 0.005	0.3270^a ± 0.009

Note: Means within a group followed by same letter are not significantly different: $p = 0.01$ and $p = 0.05$ by Duncan's multiple range tests. The values given in the table indicate the mean and standard error. $^{**}p < 0.01$, $^{*}p < 0.05$.

The results of the mean range values of the right microphone were given in Table 11. The effects of machine speed and rotor speed were not significantly important for the mean range values of the right microphone.

Table 11 Mean range values of the right microphone

Machine speed**/km h^{-1}			Rotor speed**/r min^{-1}		
*Z*1 (3.5)	*Z*2 (4.5)	*Z*3 (5.5)	*Y*1 (750)	*Y*2 (850)	*Y*3 (950)
0.3107^a ± 0.011	0.3054^a ± 0.008	0.3078^a ± 0.006	0.3079^a ± 0.018	0.3069^a ± 0.005	0.3270^a ± 0.009

Note: Means within a group followed by same letter are not significantly different: $p = 0.01$ and $p = 0.05$ by Duncan's multiple range tests. The values given in the table indicate the mean and standard error. $^{**}p < 0.01$, $^{*}p < 0.05$.

4 Conclusions

The aim of this study is to analyze noise and vibration in conventional combine harvesters using sensors. Therefore, an accelerometer was installed on each designated site in the concave. In addition, two microphones were used to register the noise of the threshing process. The results show that the effects of machine and rotor speeds were significantly important for the mean range values of the accelerometers in the *X*, *Y* and *Z* direction. It is recommended to evaluate these values with different parameters such as cutter unit position and product moisture value in future studies. The noise level of the threshing unit was determined in the study. However, in the course of operating the other systems of combine harvester, such as separating, cleaning and transmission units the noise level must be determined. The data obtained from these studies support the studies for determining the accumulation and density in advance in the combine harvester. New studies should be carried out on the basis of these values in the future in the matter of using autonomous combine harvesters.

[References]

[1] Auernhammer H, Demmel M, Muhr K, Rottmeier J, Wild K. Yield measurements on combine harvesters. ASAE Paper, 93-1506, 1993.

[2] Kutzbach H D, Wacker P, Reitz P. Developments in European combine harvesters. In Proc. AgEng, 1996, Paper No 96A–069. European Society of Agricultural Engineers.

[3] Kutzbach H D. Trends in power and machinery. J. Agric. Eng. Res, 2000; 76: 237–247.

[4] Maertens K. Data-driven techniques for the on-the- go evaluation of separation process in combine harvesters. PhD thesis, Katholieke University Leuven, 2004.

[5] Ebrahimi R, Esfahanian M, Ziaei-Rad S. Vibration modeling and modification of cutting platform in a harvest combine by means of operational modal analysis (OMA). Measurement, 2013; 46(10): 3959–3967.

[6] Hostens I, Ramon H. Descriptive analysis of combine cabin vibrations and their effect on the human body. Journal of Sound and Vibration, 2003; 266(3): 453–464.

[7] Jerath K, Brennan S, Lagoa C. Bridging the gap between sensor noise modeling and sensor characterization. Measurement, 2018; 116: 350–366.

[8] Maertens K., Ramon H, De Baerdemaeker J. An on-the-go monitoring algorithm for separation processes in combine harvesters. Comput. Electron., Agric., 2004; 43(3): 197–207.

[9] Qiu Q, Lau D. Measurement of structural vibration by using optic-electronic sensor. Measurement, 2018; 117: 435–443.

[10] Pan J, Zhang C, Zhang X. Real-time accurate odometer velocity estimation aided by accelerometers. Measurement, 2016; 91: 468–473.

[11] Feng L, Chen W, Wu T, Wang H, Dai D, Wang D, et al. An improved sensor system for wheel force detection with motion-force decoupling technique. Measurement, 2018; 119: 205–217.

[12] Xu L Z, Chai X Y, Gao Z P, Li Y M, Wang Y D. Experimental study on driver seat vibration characteristics of crawler-type combine harvester. Int J Agric & Biol Eng, 2019; 12(2): 90–99

[13] Zhang L, Zhang H D, Chen Y D, Dai S H, Li X M, Imou K, et al. Real-time monitoring of optimum timing for harvesting fresh tea leaves based on machine vision. Int J Agric & Biol Eng, 2019; 12(1): 6–9.